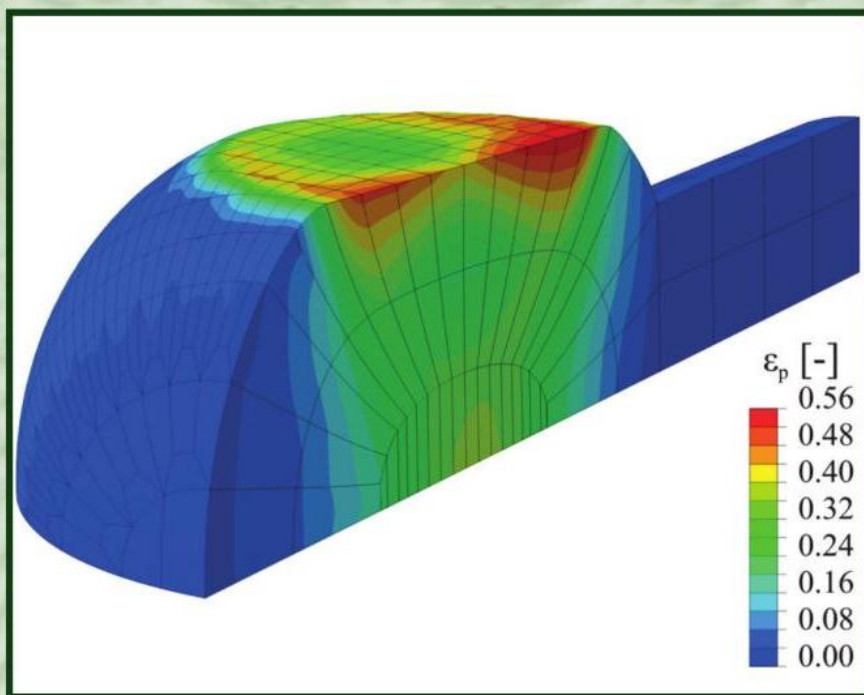


Advanced Computational Engineering and Experimenting



Edited by
Andreas Öchsner
Lucas F.M. da Silva
Holm Altenbach

Advanced Computational Engineering and Experimenting

Edited by
Andreas Öchsner
Lucas F.M. da Silva
Holm Altenbach

Advanced Computational Engineering and Experimenting

Selected, peer reviewed papers from the
Fourth International Conference on
Advanced Computational Engineering and Experimenting
(ACE-X 2010)
July 8th-9th, 2010,
Held at Hotel Concorde La Fayette Paris, France

Edited by

**Andreas Öchsner, Lucas F.M. da Silva
and Holm Altenbach**



Copyright © 2011 Trans Tech Publications Ltd, Switzerland

All rights reserved. No part of the contents of this publication may be reproduced or transmitted in any form or by any means without the written permission of the publisher.

Trans Tech Publications Ltd
Kreuzstrasse 10
CH-8635 Durnten-Zurich
Switzerland
<http://www.ttp.net>

Volume 478 of
Key Engineering Materials
ISSN 1013-9826
Full text available online at <http://www.scientific.net>

Distributed worldwide by

Trans Tech Publications Ltd.
Kreuzstrasse 10
CH-8635 Durnten-Zurich
Switzerland

Fax: +41 (44) 922 10 33
e-mail: sales@ttp.net

and in the Americas by

Trans Tech Publications Inc.
PO Box 699, May Street
Enfield, NH 03748
USA

Phone: +1 (603) 632-7377
Fax: +1 (603) 632-5611
e-mail: sales-usa@ttp.net

Preface

This special issue of Key Engineering Materials contains selected refereed papers presented at the Fourth International Conference on Advanced Computational Engineering and Experimenting (ACE-X 2010) held at the Hotel Concorde La Fayette Paris, France during the period 8th-9th July, 2010.

The goal of the conference was to provide a unique opportunity to exchange information, to present the latest results as well as to review the relevant issues on contemporary research in mechanical engineering. Young scientists were especially encouraged to attend the conference and to establish international networks with well-known scientists.

During the conference, special sessions related to *SCIENTIFIC VISUALIZATION AND IMAGING SYSTEMS* (organised by Prof. Fabiana R. Leta), *ADHESIVE BONDING* (organised by Dr. Lucas F.M. da Silva and Prof. Jean-Yves Cognard), *BIOMECHANICS* (organised by Prof. Saied Darwish), *DAMAGE AND FRACTURE OF COMPOSITE MATERIALS AND STRUCTURES* (organised by Prof. M.N. Tamin), *NUMERICAL MODELING OF MATERIALS UNDER EXTREME CONDITIONS* (organised by Prof. Nicola Bonora and Dr. Eric N Brown) were held. In addition, two short courses related to *ELASTO-PLASTIC MATERIAL BEHAVIOUR: CONTINUUM MECHANICAL MODELLING AND FINITE ELEMENT IMPLEMENTATION* (organised by Prof. Holm Altenbach and Prof. Andreas Öchsner), and *PREDICTING THE DURABILITY OF ADHESIVE BONDED JOINTS* (organised by Dr. Ian A. Ashcroft) were organised.

More than 283 scientists and researchers coming from more than 54 countries attended the conference. The large number of presented papers emphasises the considerable academic and industrial interest in the conference theme. The editors wish to thank the authors and delegates for their participation and cooperation, which made this sixth conference especially successful.

Finally, we wish to express our warm thanks and appreciation to our colleagues and associates for their sustained assistance, help and enthusiasm during the preparation of the conference.

The fifth conference, ACE-X-2011, will be held in Algarve, Portugal, from 3-6 July, 2011 (<http://www.ace-x2011.com/>).

March 2011

Andreas Öchsner
Lucas F.M. da Silva
Holm Altenbach

Table of Contents

Preface

Production of Magnesium Titanate-Based Nanocomposites via Mechanochemical Method A. Fahami, R. Ebrahimi-Kahrizsangi and B. Nasiri-Tabrizi	1
Simultaneously Synthesis and Encapsulation of Metallic Nanoparticles Using Linear–Dendritic Block Copolymers of Poly(ethylene glycol)-Poly(citric acid) A. Tavakoli Naeni, M. Vossoughi and M. Adeli	7
Study of the Properties of Al₂O₃-Ag Nanopowders Produced by an Innovative Thermal Decomposition–Reduction and Silver Nitrate Reduction Methods A.M. Jastrzębska, A.R. Kunicki and A.R. Olszyna	13
Mechanical and Microstructural Properties of Cement Paste Incorporating Nano Silica Particles with Various Specific Surface Areas A.R. Khaloo, A.G. Vayghan and M. Bolhassani	19
Improvement of the Corrosion Resistance for the Galvanic Coupling of Steel with Polypyrrole Coated Galvanized Steel A.H. El-Shazly and H.A. Al-Turaif	25
Experimental Characterization of Hydrogen Embrittlement in API 5L X60 and API 5L X80 Steels B.A. Araújo, G.D. Travassos, A.A. Silva, E.O. Vilar, J.P. Carrasco and C.J. de Araújo	34
Corrosion Monitoring in Marine Environment Using Wavelet Description I. Kuzmanić, I. Vujović and J. Šoda	40
Experimental and FEM Analysis of the AA 6082 Processed by Equal Channel Angular Extrusion J. León, C.J. Luis-Pérez, D. Salcedo, I. Pérez, J.P. Fuertes, I. Puertas and R. Luri	46
A Probabilistic Approach to the Simulation of Non-Linear Stress-Strain Relationships for Oriented Strandboard Subject to In-Plane Tension A.T. McTigue and A.M. Harte	54
Generalized Maxwell Model as Viscoelastic Lubricant in Journal Bearing M. Guemmadi and A. Ouibrahim	64
Comparative Analysis of Vaporization Rates of 5456 Aluminum Alloying Elements during CO₂ Laser Welding J.I. Achebo and O. Oghoore	70
Analysis of Chip Damage Risk in Thermosonic Wire Bonding C. Dresbach, G. Lorenz, M. Petzold and H. Altenbach	75
Free Vibration Characteristics of Thermally Loaded Rectangular Plates B.H. Jeon, H.W. Kang and Y.S. Lee	81
Structure-Property Relationship of Burn Collagen Reinforcing Musculo-Skeletal Tissues Y.L. Yeo, K.L. Goh, L. Kin, H.J. Wang, A. Listrat and D. Bechet	87
Femur Design Parameters and Contact Stresses at UHMWPE Hip Joint Cup H. Fouad and S.M. Darwish	93
Biomechanical Characterization of a Cervical Corporectomy Using Porcine Specimens, Following an Experimental Approach L.H. Hernández-Gómez, J.A. Beltrán-Fernández, G. Urriolagoitia-Calderón, A. González-Rebatú, M.M. Galán Vera and G. Urriolagoitia-Sosa	103

Production of Magnesium Titanate-Based Nanocomposites via Mechanochemical Method

Abbas Fahami^a, Reza Ebrahimi-Kahrizsangi^b, Bahman Nasiri-Tabrizi^c

Materials Engineering Department, Islamic Azad University, Najafabad Branch, Isfahan, Iran

^aa.fahami@hotmail.com, ^brezaeabrahimi@iaun.ac.ir, ^cbahman_nasiri@hotmail.com

Key words: Magnesium titanate, Hydroxyapatite, Whitlockite, Mechanical alloying, Nanocrystalline, Structural features.

Abstract. The mechanical activation was employed to study the phase evolution of the Mg–TiO₂–CaHPO₄–CaO nanocrystalline system. The powders mixture with certain weight percent was grinded. Thermal annealing process at 650°C, 900°C and 1100°C temperatures resulted in generation of different compounds like MgTiO₃/MgO/Hydroxyapatite (HAp) and MgTiO₃/MgO/ β -TCP and MgTiO₃/Mg₂TiO₄/MgO/ β -TCP, respectively. The compounds were characterized by X-ray diffraction (XRD), scanning electron microscopy (SEM), transmission electron microscopy (TEM), and energy dispersive X-ray spectroscopy (EDX). The consequences of XRD analysis revealed that by increasing temperature, some composites with different morphological and structural features were detected. Beside, due to decomposing of HAp around 800°C, HAp converted to whitlockite (β -TCP) with growth of temperature. According to SEM and TEM observations, it was found that the synthesized powder contained large agglomerates which significant content of finer particles and agglomerates with spherical morphology. Because magnesium titanates based dielectric materials are useful for electrical applications, the electrical property of HAp has been proved, and the incorporation of these materials could result in new nanocrystalline dielectric materials.

Introduction

The preparation and characterization of nano-dielectric materials have attracted increasing attention in the last two decades [1]. Nanostructured materials exhibit unusual physical and chemical properties, significantly different from those of conventional materials, due to their extremely small size or large specific surface area [2].

Magnesium titanates are important as dielectric ceramic industrial materials. There are three intermediate phases between MgO and TiO₂ such as qandilite (Mg₂TiO₄), geigielite (MgTiO₃), and karrooite (MgTi₂O₅). The formation of these phases depends on the relative stoichiometry of materials in the precursor [3]. The geigielite and qandilite, due to their dielectric properties like low dielectric loss (high quality factor), high dielectric constant, and near zero temperature coefficient of resonant frequency [4,5], have widespread applications in resonators, pigments, filters, antennas for communication, radar, direct broadcasting satellite and global positioning system operating at microwave frequencies and in the electrical and electronic industries as a dielectric material for manufacturing on-chip capacitors, high frequency capacitors and temperature compensating capacitors [6]. Various methods for the preparation of magnesium titanates microcrystalline powders were reported including solid state reactions [7], co-precipitation [8], and thermal decomposition of peroxide precursors [9], mechanochemical complexation [10], and sol–gel route [11]. On the other hand, the most important calcium phosphate based nanocomposites comprised of HAp and β -TCP. In addition of the good biocompatibility of HAp, the dielectric properties of these bioceramics have been evaluated in numerous studies [12-14]. Also, it has been found that such properties of HAp are greatly affected by various parameters such as Ca/P ratio and sintering temperature [15]. However, precise investigation is demanded for these compounds in the future.

Nowadays, the various methods like chemical precipitation [16], hydrothermal [17] and microwave irradiation [18] have been used to synthesize of calcium phosphate-based ceramics. Among different dry processes, mechanical alloying (MA) [19] is one of the most current methods for manufacturing of dielectric ceramics.

In this paper, the phase transformation of the Mg–TiO₂–CaHPO₄–CaO nanocrystalline system is investigated. Also the preparation of MgTiO₃/MgO/HAp, MgTiO₃/MgO/ β -TCP and MgTiO₃/Mg₂TiO₄/MgO/ β -TCP nanocomposites through mechanical activation and subsequent thermal treatment are studied. In fact, the aim of this work is to discuss the synthesis and structural evaluation of the nanocomposites. The dielectric properties of MgTiO₃, Mg₂TiO₄ and MgO and their effective applications in electric equipments have been proven [20]. In addition, HAp has such as these characteristics as well [15]. For all these reasons, compound of these materials could be derived to create new nanocrystalline dielectric materials.

Experimental Procedures

Preparation Method. Fig. 1 depicts the flow chart for the synthesis of various nanocomposites by mechanical activation and subsequent thermal annealing. Calcium hydrogen phosphate (CaHPO₄, Merck $\geq 98\%$), calcium oxide (CaO, Merck), titanium oxide (TiO₂, Merck), and magnesium (Mg, Merck) were the starting reactant materials for the MA processing. In order to prepare the composites, a distinct amount of calcium hydrogen phosphate and calcium oxide (Ca/P = 1.67) blend (20 wt.%) was milled with a mixture of titanium oxide and magnesium for 60 h and subsequent thermal treatments were performed in an electrical furnace at 650°C, 900°C and 1100°C for 2 h in air. The powder mixture with the desired stoichiometric proportionality was milled by a high energy planetary ball mill under ambient air atmosphere. The grinding process was performed in polymeric vial using Zirconia balls (diameter 20 mm). The charge to ball ratio and rotational speed were 1:20 and 600 rpm, respectively.

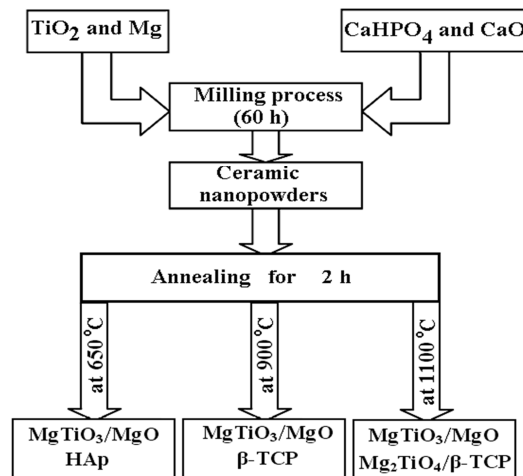


Fig. 1 Flow chart for the synthesis of magnesium titanate- based nanocomposites by mechanochemical method and subsequent heat treatment.

Characterization Techniques. Phase identification was carried out by XRD analysis with Xpert-Philips diffractometer using *Cu K α* radiation. The diffractometer was operated at 40 kV and 30 mA. All measurements were performed at room temperature with the diffraction range of $2\theta = 10^\circ - 80^\circ$ at $1^\circ/\text{sec}$ speed. The diffraction patterns of products were compared to proposed standards by the Joint Committee on Powder Diffraction and Standards (JCPDS), which involved card # 003-0747 for HAp, # 003-0713 for Ca₃(PO₄)₂, # 006-0494 for MgTiO₃, # 025-1157 for Mg₂TiO₄, # 021-1272 for TiO₂, # 004-0829 for MgO, and # 037-1497 for CaO. Energy dispersive X-ray spectroscopy (EDX) which is coupled to SEM was used to the semi-quantitative examination of the synthesized powders. Scanning electron microscope (SEM, SERON AIS-2100) was applied to characterize the morphological characteristics of the samples which were sputter-coated with a thin layer of gold. The size and morphology of the fine powders were observed in a transmission electron microscope (Philips CM10).

Results and Discussions

XRD Analyses. Fig. 2 (a-b) shows spectra of XRD patterns which belong to milled mixtures and subsequent thermal annealing powders, respectively. Fig. 2a, illustrates the peaks that is significant for TiO_2 and MgO and MgTiO_3 .

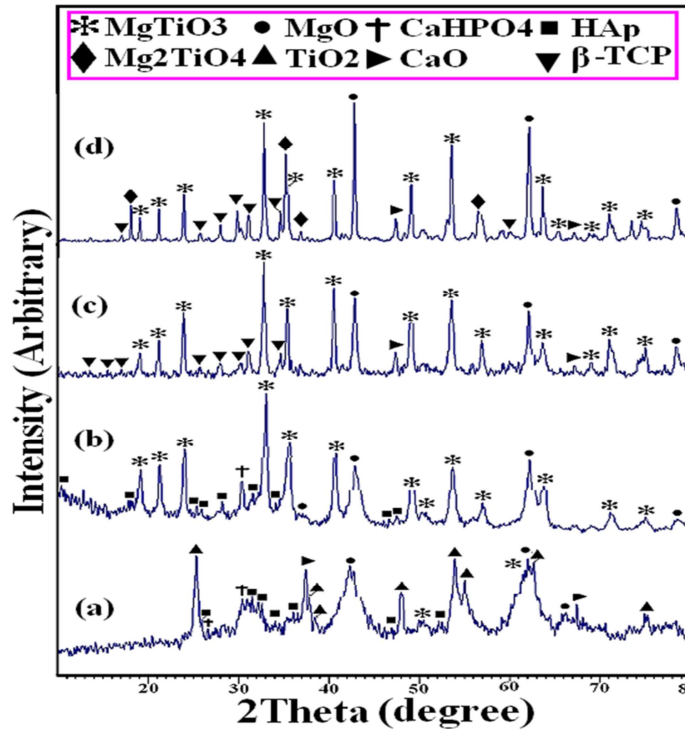


Fig. 2 XRD patterns of nanocomposites milled powders (a) and heat treated at different temperatures, (b) 650 °C (c) 900 °C and (d) 1100 °C.

It should be noted that the presence of MgTiO_3 in milled powder indicate that milling during 60 h can lead to the formation of magnesium titanates phases such as MgTiO_3 (geigielite), Mg_2TiO_4 (qandilite), and MgTi_2O_5 (karrooite). On the other hand, a few certain peaks exist which are representative for HAp. It indicates that CaO was reacted with CaHPO_4 according to reaction (1).



The XRD patterns of milled powder after annealing at 650 °C, 900 °C and 1100 °C are displayed in Fig.2 (b-d). According to Fig. 2b, the heat treated sample at 650 °C produced a $\text{MgTiO}_3/\text{MgO}/\text{HAp}$ nanocomposite. It shows that TiO_2 has reacted with MgO which formed MgTiO_3 . Hence, HAp and some of the magnesia has remained intact. By increasing temperature till 900 °C, MgTiO_3 and MgO have remained sharply but according to reaction (2) HAp was decomposed and converted to $\beta\text{-TCP}$ and CaO . The XRD analysis of this sample is shown in Fig. 2c.



It is reported in [21] that the decomposition temperature (600–800 °C) strongly depends on the preparation method of the HAp powder. As shown in Fig. 2d, thermal treatment at 1100 °C leads to formation of a $\text{MgTiO}_3/\text{Mg}_2\text{TiO}_4/\text{MgO}/\beta\text{-TCP}$ nanocomposite. Since, qandilite and karrooite are stable at high temperature, some magnesia and geigielite have reacted together and formed qandilite (reaction 3).



Based on XRD patterns of the heat treated samples, the width of the peaks become narrower as compared to the results for the milled powder which shows an increase in the degree of crystallinity.

SEM-EDX Analyses. The SEM micrographs of the samples after the milling and annealing processes are shown in Fig. 3. The SEM micrographs show that particles of products can be attached at crystallographically specific surfaces and form elongated agglomerates composed of many primary crystallites. In fact, the chemical interactions at the contacting surface of particles result in very compact particles forming large agglomerates with spheroidal morphology. Based on Fig. 3a the mean size of the powder particles decreases after 60 h of milling. On the other hand, the mean size of the milled powder particles increases after annealing at 650°C, 900°C, and 1100°C. However, only a slight change in particle size is observed in these samples (Fig. 3 b-d). As temperature increases, the SEM micrographs show a continuous evolution of the morphological features. In fact, the mean size of the powder particles increases after the annealing process. Moreover, with an increase of the annealing temperature from 650°C to 1100°C the spheroidal particles become considerably large in size. Fig.4 (a-d) displays the concentrations of elements by the EDX spectra. The results of EDX analyses indicate a higher Mg/Ti ratio in small area of EDX analysis compared to Ca/P ratio which agrees with the chemical composition of the powder mixture. Furthermore, chemically stable contaminants are not detected due to the excessive adhesion of powders to the vial and balls.

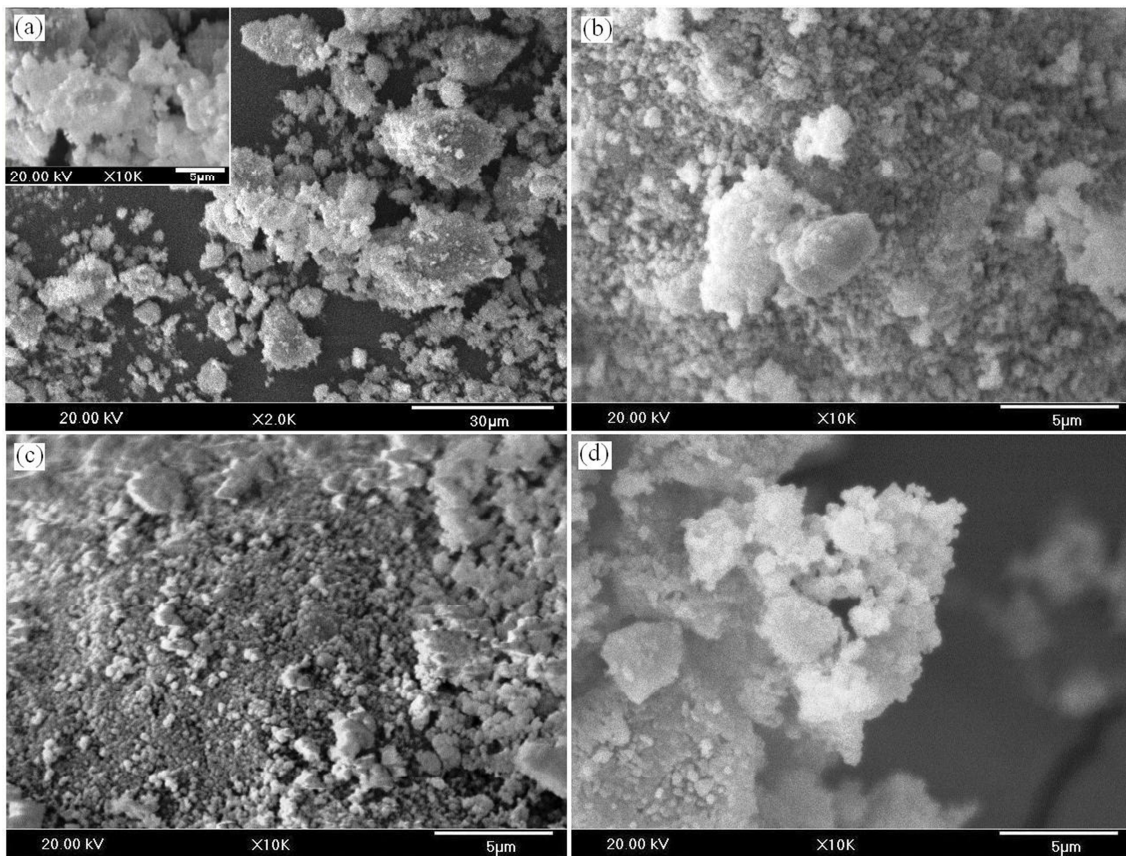


Fig. 3 SEM micrographs of nanocomposites (a) mixed powder and heat treated at different temperatures, (b) 650°C (c) 900°C and (d) 1100°C.

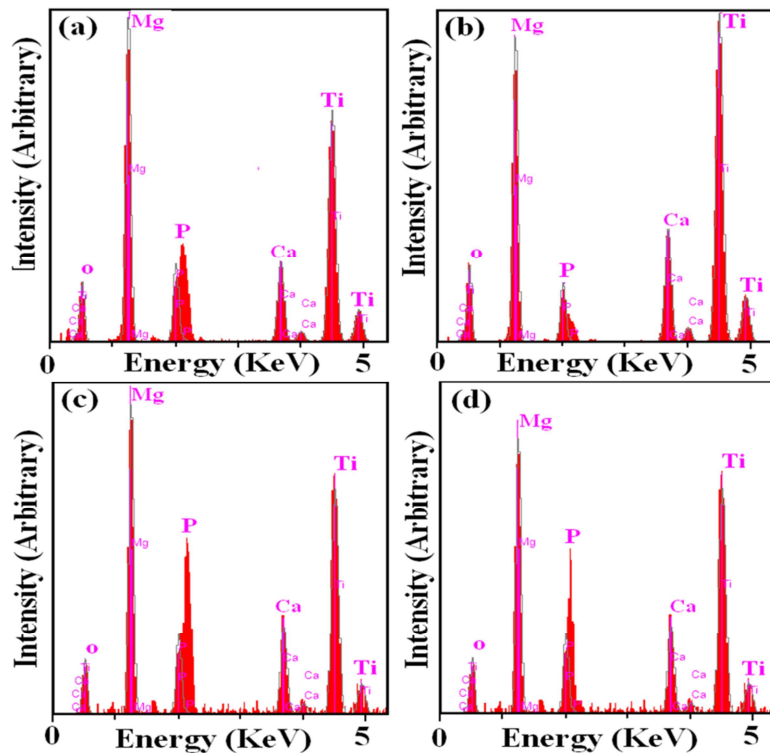


Fig. 4 EDX analysis of nanocomposites mixed powder (a) and heat treated at different temperatures, (b) 650°C (c) 900°C and (d) 1100°C.

TEM Analyses. Fig. 5 (a) and (b) shows the transmission electron images of milled powder after 60 h and a heat treated sample at 1100°C for 2 h. In Fig. 5a, it can be seen that the agglomerates (100 nm in size) are formed after milling. The agglomerates consist of radially attached fibers. Also, Fig. 5b shows a growth of the powder particle after annealing at 1100°C which agrees with the data obtained from the SEM micrographs. It is revealed that particles with spheroidal shapes are formed after the thermal annealing process.

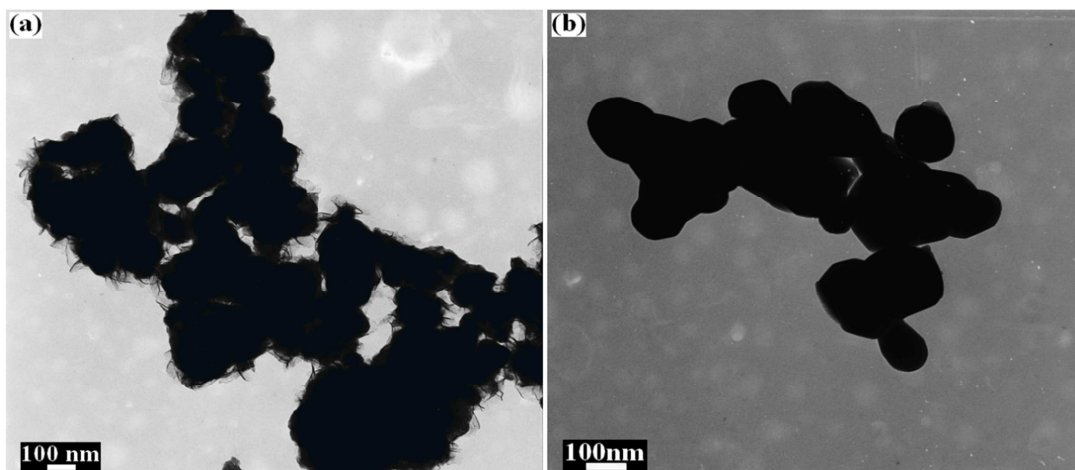


Fig. 5 TEM images of (a) milled sample and (b) heat treated sample at 1100°C.

This is the first report of the preparation of $\text{MgTiO}_3/\text{MgO}/\text{HAp}$, $\text{MgTiO}_3/\text{MgO}/\beta\text{-TCP}$, and $\text{MgTiO}_3/\text{Mg}_2\text{TiO}_4/\text{MgO}/\beta\text{-TCP}$ nanocomposites and, therefore, there is no directly comparable data in the literature. However, further work is needed to investigate the electrical properties and identify optimal HAp and $\beta\text{-TCP}$ levels that satisfy electrical performance criteria. Other properties and electrical performance of these nanostructured materials will be carried out in our research center.

Conclusions

In this work, we have investigated the phase transformation in a Mg–TiO₂–CaHPO₄–CaO system. Based on XRD analysis, the presence of MgTiO₃ in milled powder indicates that the mechanical activation during 60 h can lead to the formation of magnesium titanates phases and thermal annealing of the milled powders at various temperatures resulted in the formation of three different nanocomposites. According to evaluations of the structural and morphological features, the best annealing temperature for the MgTiO₃ based nanocomposites is 650°C. SEM and TEM micrographs show that the crystal growth behavior of compounds depends on thermal annealing temperatures. The results confirmed that the solid state combination in polymeric vial and appropriate thermal annealing process is a suitable route to produce commercial amount of magnesium titanate nanocomposites.

References

- [1] N. Stubicar, A. Tonejc and M. Stubicar: *J. Alloys Compd.* Vol. 370 (2004), p. 296.
- [2] C.L. De Castro, B.S. Mitchell, in: *Synthesis, functionalization and surface treatment of nanoparticles*, Baraton MI, editors, chapter, American Scientific Publishers (2002).
- [3] K. Hamada, Sh.I. Yamamoto and M. Senna: *Adv. Powder Technol.* Vol. 11 (2000), p.361.
- [4] D. Li, L. Wang and D. Xue: *J. Alloys Compd.* Vol. 492 (2010), p. 564.
- [5] M. Valant, M. Macek-Krzmanec and D. Suvorov: *J. Eur. Ceram. Soc.* Vol. 27 (2007), p. 2963.
- [6] N. Dharmaraj, H.C. Park, B.M. Lee, P. Viswanathamurthi, H.Y. Kim and D.R. Lee: *Inorg. Chem. Commun.* Vol. 7 (2004), p. 431.
- [7] B. Wechsler, A. Navrotsky: *J. Solid State Chem.* Vol. 55 (1984), p. 165.
- [8] M.J. Martinez-Lope, M.P. Baura-Pena and M.E. Garcia-Clavel: *Thermochim. Acta* Vol. 194 (1992), p. 247.
- [9] G. Pfaff: *Ceram. Int.* Vol. 20 (1994), p. 111.
- [10] J. Liao, M. Senna, *Mater. Res. Bull.* Vol. 30 (1995), p. 385.
- [11] I.R. Abothu, A.V. Prasada Rao and S. Komarneni: *Mater. Lett.* Vol. 38 (1999), p. 186.
- [12] M.A. Fanovich, M.S. Castro and J.M. Porto Lopez: *Ceram. Int.* Vol. 25 (1999), p. 517.
- [13] T. Ikoma, A. Yamazaki, S. Nakamura and M. Akao: *J. Mater. Sci. Lett.* Vol. 18 (1999), p. 1225.
- [14] M.S. Khalil, H.H. Beheri and W.I. Abdel Fattah: *Ceram. Int.* Vol. 28 (2002), p. 451.
- [15] M. Quilitz, K. Steingrover and M. Veith: *J. Mater. Sci. - Mater. Med.* Vol. 21 (2009), p.399.
- [16] Y. Liu, W. Wang, Y. Zhan, C. Zheng and G. Wang: *Mater. Lett.* Vol. 56 (2002), p. 496.
- [17] K. Lin, J. Chang, R. Cheng and M. Ruan: *Mater. Lett.* Vol. 61 (2007), p. 1683.
- [18] A.L. Macipe, J.G. Morales and R.R. Clemente: *Adv. Mater.* Vol. 10 (1998), p. 49.
- [19] S.H. Rhee: *Biomaterials* Vol. 23 (2002), p. 1147.
- [20] I.R. Abothu, A.V. Prasada Rao and S. Komarneni: *Mater. Lett.* Vol. 38 (1999), p. 186.
- [21] M.H. Fathi, A. Hanifi: *Mater. Lett.* Vol. 61 (2007), p. 3978.

Simultaneously Synthesis and Encapsulation of Metallic Nanoparticles using Linear–Dendritic Block Copolymers of Poly (ethylene glycol)-Poly (citric acid)

Ashkan Tavakoli Naeini^{1,4,a}, Manouchehr Vossoughi^{1,2,b}, Mohsen Adeli^{2,3,c}

¹Department of Chemical and Petroleum Engineering, Sharif University of Technology, Tehran, Iran

²Institute for Nanoscience and Nanotechnology, Sharif University of Technology, Tehran, Iran

³Department of Chemistry, Sharif University of Technology, Tehran, Iran

⁴Biochemical and Bioenvironmental Engineering Research Center, Sharif University of Technology, Tehran, Iran

^aashkan.tavakolin@gmail.com, ^bvosoughi@sharif.edu, ^cmohadeli@yahoo.com

Key words: Encapsulation, Block copolymer, Gold nanoparticles, Silver nanoparticles, Loading capacity

Abstract. Linear-dendritic triblock copolymers of linear poly(ethylene glycol) and hyperbranched poly(citric acid) (PCA-PEG-PCA) were used as the reducing and capping agents to encapsulate gold and silver nanoparticles (AuNPs and AgNPs). PCA-PEG-PCA copolymers in four different molecular weights were synthesized using 2, 5, 10 and 20 citric acid/PEG molar ratios and were called A₁, A₂, A₃ and A₄, respectively. Nanoparticles were encapsulated simultaneously during the preparation process. AuNPs were simply synthesized and encapsulated by addition a boiling aqueous solution of HAuCl₄ to aqueous solutions of A₁, A₂, A₃ and A₄. In the case of silver, an aqueous solution of AgNO₃ was reduced using NaBH₄ and AgNPs were encapsulated simultaneously by adding aqueous solutions of different PCA-PEG-PCA to protect the fabricated silver nanoparticles from aggregation. Encapsulated AuNPs and AgNPs were stable in water for several months and agglomeration did not occur. The synthesized silver and gold nanoparticles have been encapsulated within PCA-PEG-PCA macromolecules and have been studied using Transmission Electron Microscopy (TEM) and UV/Vis absorption spectroscopy. Studies reveal that there was a reverse relation between the size of synthesized AuNPs/AgNPs and the size of citric acid parts of PCA-PEG-PCA copolymers. For example, the prepared gold and silver nanoparticles by A₃ copolymer are of an average size of 8 nm and 16 nm respectively. Finally, the loading capacity of A₁, A₂, A₃ and A₄ and the size of synthesized AuNPs and AgNPs were investigated using UV/Vis data and the corresponding calibration curve. It was found that the loading capacity of copolymers depends directly on the concentration of copolymers and their molecular weight.

Introduction

Synthesis of metallic nanoparticles and the study of their size and properties is of fundamental importance in the advancement of recent research [1,2,3]. It is found that the optical, electronic, magnetic, and catalytic properties of metallic nanoparticles depend on their size, shape and chemical surroundings [2,3]. In nanoparticle synthesis it is very important to control not only the particle size but also the particle shape and morphology. Properties of metallic nanoparticles are different from those of bulk materials made from the same atoms. For example, the striking effect of nanoparticles on color has been known since antiquity when tiny metal particles were used to color glass in church windows. Silver particles stained the glass yellow, while gold particles were used to make ruby-colored glass. Nanogold or gold nanoparticles (AuNPs) have been widely studied in the past 10 years because of their unique properties, such as catalysis, quantum size